Journal of King Saud University – Science (2014) **26**, 222–229

King Saud University
Journal of King Saud University – Science
www.ksu.edu.sa
www.sciencedirect.com

ORIGINAL ARTICLE

Biomimetic synthesis of silver nanoparticles using the amphibious weed ipomoea and their application in pollution control

S.U. Ganaie, Tasneem Abbasi [1], J. Anuradha, S.A. Abbasi *

Center for Pollution Control and Environmental Engineering, Pondicherry University, Puducherry 605014, India

Received 22 November 2013; accepted 21 February 2014
Available online 20 March 2014

KEYWORDS

Biomimetic synthesis;
Silver nanoparticles;
Ipomoea;
Alizarin Red S;
Remazol Brilliant Blue R

Abstract Use of aqueous extracts of leaves, stems, and roots of the pernicious aquatic weed ipomoea (*Ipomoea carnea*) drawn from different locations was explored in the biomimetic extracellular synthesis of silver nanoparticles (SNPs). It was found that despite the natural variability in the chemical content of ipomoea growing in different locations, certain extract–metal stoichiometries can be identified which give strikingly reproducible results in terms of the size and the shape of the SNPs. This is one of the first reports of its type in which possible role of natural variability in the chemical composition of a given botanical species on nanoparticle synthesis involving that species has been assessed.

The use of the SNPs was explored in the degradation of typical organic pollutants—the dyes Alizarin Red S and Remazol Brilliant Blue R. The SNPs were found to speed up the dye degradation.

1. Introduction

These authors (Abbasi et al., 2012a,b) have recently established the feasibility of using aqueous extracts of the highly pernicious and dominant weed ipomoea (*Ipomoea carnea*) in generating silver nanoparticles (SNPs). It is a biomimetic procedure because it mimes the way in which chemicals present in the body of ipomoea reduce metal ions to nanoparticles and then stabilize those nanoparticles by forming a coating around them. Whereas in nature this happens within the plant cells, these authors achieve it extracellularly by first bringing those chemicals into an aqueous extract of the relevant plant part and then make portions of the extract react with Ag (I). Unlike several other bottom-up approaches of nanoparticle generation which are based either on chemical synthesis or the use of microorganisms, plant-based biomimetic methods consume very little energy, generate very little pollution (if any), and mostly operate under conditions of normal temperature and pressure (Anuradha et al., 2010, 2011a; Awwad et al., 2013; Bhat et al., 2013; Dubey et al., 2013; Kumar et al., 2012, 2013; Kotakadi et al., 2014; Nazeruddin et al., 2014). The state-of-the-art has been summarized from time to time (Anuradha et al., 2011, 2014). Plant-based methods also do not require sophisticated controls in maintaining the bioagent

* Corresponding author.
E-mail address: abbasi.cpee@gmail.com (S.A. Abbasi).
[1] Concurrently Visiting Associate Professor, Worchester Polytechnic Institute, USA.
Peer review under responsibility of King Saud University.

ELSEVIER Production and hosting by Elsevier

1018-3647 © 2014 Production and hosting by Elsevier B.V. on behalf of King Saud University.
http://dx.doi.org/10.1016/j.jksus.2014.02.004

as are necessitated in the case of microorganisms. In this respect they represent an advantage similar to the other 'green' procedures that are emerging, such as microwave-assisted nanoparticle synthesis (Dahl et al., 2007; Raspolli Galletti et al., 2008, 2009, 2010, 2012, 2013). Moreover, by using ipomoea as the main bioagent, the authors have achieved several additional advantages:

(a) Ipomoea is a freely available weed which has no beneficial uses at present. Hence this manner of utilization of ipomoea does not compete with its any other use. In contrast, most past attempts to biomimetically synthesize SNPs have relied on botanical species which have numerous other beneficial uses as a food item (Antony et al., 2013), a source of cosmetics/medicines (Anuradha et al., 2011b; Gavhane et al., 2012, or an ornamental plant (Kumar et al., 2013; Dubey et al., 2013).
(b) Any process which can gainfully utilize ipomoea has the great advantage that it would contribute to the mechanical removal of ipomoea, thereby effecting some control over the weed's spread. At present, in the absence of such use, no one is interested in harvesting ipomoea resulting into its increasing colonization of land surface and wetlands (Chari et al., 2005).
(c) When it gets a chance to spread unchecked as it has in India and several other parts of the world (Meira et al., 2012; Gorniak et al., 2010), ipomoea becomes a very harmful plant in the sense that it causes toxicity to the mammals that graze upon it. It also generates toxic exudates (Ikeda et al., 2003; Hueza et al., 2005) which make the soil unfit for the growth of several other species. The weed exerts allopathic effect—it is able to discourage and prevent the growth of several species of plants in its habitat. Apart from these particularly harmful attributes, ipomoea's infestation also generates all the other negative impacts associated with the dominance of any single species: it destroys biodiversity, and it monopolizes the use of water, soil, and associated nutrients (Chari and Abbasi, 2004, 2005). When ipomoea plants die, they degrade in the open generating global warming gases CO_2 or CO_2–CH_4 mixtures, depending on whether the degradation occurs under aerobic or anaerobic conditions.

In this paper, a major step is reported which has been taken toward possible large-scale utilization of ipomoea in generating SNPs by (a) assessing how reproducible the process can be, given the natural variability that occurs in the chemical composition of any plant species that grows at different locations; and (b) assessing how best each plant part—leaves, stems, roots—can be used for the purpose so that the entire ipomoea biomass can be gainfully utilized in the process.

2. Materials and method

All glassware was thoroughly cleaned with liquid detergents and washed liberally with tap water followed by rinsing with deionized distilled water and drying in hot air oven before use. All chemicals used were of analytical reagent grade, or equivalent, unless otherwise specified.

Whole plants of ipomoea were collected from different locations in and around Puducherry. The plants were washed with tap water, saline (9% NaCl) water, and deionized distilled water. The adhering water was removed using blotting paper and the randomly picked plant parts were cut into 1–2 cm pieces and weighed. Their dry weight was determined by keeping them at 110 °C in an oven till they reached a constant weight. The total solid (TS) content was computed.

The extracts of leaves, stems, and roots were separately prepared. For this weighted quantities of the relevant plant parts were heated with measured volumes of water to ~100 °C for about 5 min in sterile distilled water in a water bath. The contents were cooled to room temperature and filtered through a nylon mesh and then by a Whatman No. 42 filter paper. The extracts thus obtained were stored at 4 °C, and used within 7 days.

A 10^{-3} M stock solution of silver nitrate was prepared and kept in amber color bottle wrapped in black plastic sheet to keep off light. Other stock solutions were prepared as needed. All ipomoea quantities as reported are on dry weight (TS) basis.

2.1. Nanoparticle synthesis

The extra-cellular biomimetic synthesis achieved by us evidently occurs in two-steps which take place in quick succession—in the first step certain biomolecules present in the plant reduce the monovalent silver ion to uncharged atoms. Then, as these atoms aggregate to reach nano-size, other biomolecules from the plant envelope or 'cap' them to prevent their further aggregation. This mechanism was proposed by the early workers in this field (Shankar et al., 2003, 2004) and nothing else has been reported so far to suggest it may not be true.

Different proportions of metal ion solutions and plant extracts, formed with the extracts of 1000, 2000, 4000, 6000, and 10,000 mg/l concentrations and metal ions at 134, 134, 134, 120, and 84 mg/l levels, respectively, (to yield metal–extract ratios of 1:7.5, 1:15, 1:30, 1:50, and 1:120, respectively), were employed to determine the effect of various stoichiometric combinations on the shapes and sizes of the resulting SNPs. This is a crucial input to process development. The reactions between the metal ion solutions and the plant extracts were all carried out at room temperature (30 ± 3 °C) without any stirring. Hence the use of energy was minimal. SNP formation was signaled by the appearance of a brownish yellow color. The progress of SNP formation was monitored spectrophotometrically over the wavelength range 190–1100 nm.

The peak wavelength (λ_{max}), the values of the absorbance (O.D.), the manner of change in the color of the reaction mixture, etc., were noted at different time intervals. These findings were then linked to HR-SEM and TEM images, FTIR spectra, EDAX, and other studies to generate information on the shapes and the sizes of the SNPs.

2.2. Catalytic reduction of typical dyes by silver nanoparticles

To study the role of SNPs in catalyzing dye-degradation, 7×10^{-4} M and 3×10^{-4} M solutions of Alizarin Red S and Remozal Brilliant Blue R, respectively, were prepared. These concentrations were employed as Beer's law was seen to be

followed in the ranges that began with these concentrations and went onto 10^{-5} M and lesser. Both stock solutions were stored in the dark. To a mixture containing 1 ml of either dye solution and 1 ml of sodium borohydride (0.001 M), 1 ml of SNP suspension was added in a reaction tube. The volume of the mixture was made up to 4 ml with water. The progress of the reaction was monitored spectrophotometrically by recording the optical density of the dye's absorption maxima. For the uncatalyzed reaction 1 ml of SNPs was replaced by an equal amount of water. In another set of studies for each

Table 1 Absorption maxima (λ_{max}) and absorbance of SNPs obtained using aqueous extracts of ipomoea leaves: effect of ipomoea source, reaction time, and metal–extract stoichiometry.

Locations	Reaction duration (hrs)	Metal–extract proportions									
		1:7.5		1:15		1:30		1:50		1:120	
		λ_{max}	Abs	λ_{max}	Abs	λ_{max}	Abs	λ_{max}	Abs	λ_{max}	Abs
I	0th	–	–	–	–	–	–	–	–	–	–
	2nd	–	–	–	–	–	–	–	–	–	–
	4th	440	0.98	440	1.38	–	–	–	–	–	–
	6th	441	1.21	442	1.66	–	–	–	–	–	–
	24th	449	2.26	459	2.68	–	–	–	–	–	–
II	0th	–	–	–	–	–	–	–	–	–	–
	2nd	–	–	–	–	–	–	–	–	–	–
	4th	439	0.90	–	–	–	–	–	–	–	–
	6th	439	1.10	–	–	–	–	–	–	–	–
	24th	441	1.75	450	0.92	–	–	–	–	–	–
III	0th	–	–	–	–	–	–	–	–	–	–
	2nd	439	0.86	437	0.99	–	–	–	–	–	–
	4th	442	1.33	442	1.61	–	–	–	–	–	–
	6th	447	1.57	443	1.79	–	–	–	–	–	–
	24th	447	2.52	443	2.48	450	0.77	–	–	–	–
IV	0th	–	–	–	–	–	–	–	–	–	–
	2nd	–	–	–	–	–	–	–	–	–	–
	4th	429	0.34	440	0.74	442	1.10	–	–	–	–
	6th	432	0.47	443	0.95	445	1.38	–	–	–	–
	24th	440	0.97	450	1.67	448	2.08	443	1.04	–	–

Table 2 Absorption maxima (λ_{max}) and absorbance of SNPs obtained using aqueous extracts of ipomoea root: effect of ipomoea source, reaction time, and metal–extract stoichiometry.

Locations	Reaction duration (hrs)	Metal–extract proportions									
		1:7.5		1:15		1:30		1:50		1:120	
		λ_{max}	Abs	λ_{max}	Abs	λ_{max}	Abs	λ_{max}	Abs	λ_{max}	Abs
I	0th	–	–	–	–	–	–	–	–	–	–
	2nd	447	0.71	450	1.28	435	0.98	–	–	–	–
	4th	451	0.91	457	1.55	440	1.29	–	–	–	–
	6th	451	1.00	456	1.71	443	1.44	–	–	–	–
	24th	460	1.57	457	2.45	456	2.28	–	–	–	–
				490	2.32						
II	0th	–	–	–	–	–	–	–	–	–	–
	2nd	–	–	–	–	–	–	–	–	–	–
	4th	444	0.65	447	0.92	–	–	–	–	–	–
	6th	445	0.84	449	1.15	–	–	–	–	–	–
	24th	447	1.49	444	1.91	–	–	–	–	–	–
III	0th	–	–	–	–	–	–	–	–	–	–
	2nd	–	–	444	0.64	–	–	–	–	–	–
	4th	–	–	448	1.09	–	–	–	–	–	–
	6th	435	0.50	456	1.34	–	–	–	–	–	–
	24th	442	0.81	449	2.13	441	1.07	–	–	–	–
IV	0th	–	–	–	–	–	–	–	–	–	–
	2nd	–	–	–	–	–	–	–	–	–	–
	4th	429	0.34	440	0.74	442	1.10	–	–	–	–
	6th	432	0.47	443	0.95	445	1.38	–	–	–	–
	24th	440	0.97	450	1.67	448	2.08	443	1.04	–	–

dye, hydrogen peroxide (0.1 M) was used instead of sodium borohydride for the dye degradation with or without SNP catalyst.

3. Results and discussion

3.1. Effect of natural variability in the chemical content of ipomoea on the SNP formation

The spectral characteristics of the SNPs formed—as influenced by the variety of ipomoea, reaction time, and the stoichiometry—for ipomoea leaves are summarized in Table 1. As may be seen, at lower extract–metal ratios, SNP formation commences in 4 h in ipomoea drawn from locations I, II, and IV while in ipomoea belonging to location III it occurs in 2 h. Hence, it can be said, that in general, and independent of the ipomoea source, SNP formation by this process would commence in about 4 h from the time of mixing the reactants.

Extracts prepared from the roots of ipomoea plants derived from different locations also gave fairly reproducible results, especially in terms of positions of the absorption peaks (Table 2); similar were the findings when stem extract was used, with the exception that no SNP formation was seen at 1:30 and higher Ag(I)-extract concentrations (Table 3).

The spectra of SNPs formed in 1:7.5 and 1:15 metal–extract combinations were remarkably similar in terms of peak position and strength in all locations, even as there were differences in the rate and characteristics of SNPs formed by different plant parts (Table 4). This indicates that the shapes and sizes of SNPs can be controlled and reproduced by controlling metal–extract proportions, and choosing appropriate plant parts, irrespective of the natural variability in the chemical content of ipomoea.

Table 3 Absorption maxima (λ_{max}) and absorbance of SNPs obtained using aqueous extracts of ipomoea stem: effect of ipomoea source, reaction time, and metal–extract stoichiometry.

Location	Reaction duration (in hrs)	Metal–extract proportions									
		1:7.5		1:15		1:30		1:50		1:120	
		λ_{max}	Abs	λ_{max}	Abs	λ_{max}	Abs	λ_{max}	Abs	λ_{max}	Abs
I	0th	–	–	–	–	–	–	–	–	–	–
	2nd	–	–	–	–	–	–	–	–	–	–
	4th	446	0.85	–	–	–	–	–	–	–	–
	6th	449	1.01	–	–	–	–	–	–	–	–
	24th	461	1.63	490	1.26	–	–	–	–	–	–
II	0th	–	–	–	–	–	–	–	–	–	–
	2nd	–	–	–	–	–	–	–	–	–	–
	4th	443	0.18	–	–	–	–	–	–	–	–
	6th	445	1.40	–	–	–	–	–	–	–	–
	24th	447	1.98	470	1.41	–	–	–	–	–	–
III	0th	–	–	–	–	–	–	–	–	–	–
	2nd	465	0.88	–	–	–	–	–	–	–	–
	4th	461	1.17	–	–	–	–	–	–	–	–
	6th	459	1.36	–	–	–	–	–	–	–	–
	24th	456	1.96	465	1.39	–	–	–	–	–	–
IV	0th	–	–	–	–	–	–	–	–	–	–
	2nd	–	–	–	–	–	–	–	–	–	–
	4th	433	0.29	–	–	–	–	–	–	–	–
	6th	435	0.42	–	–	–	–	–	–	–	–
	24th	440	0.87	456	0.68	–	–	–	–	–	–

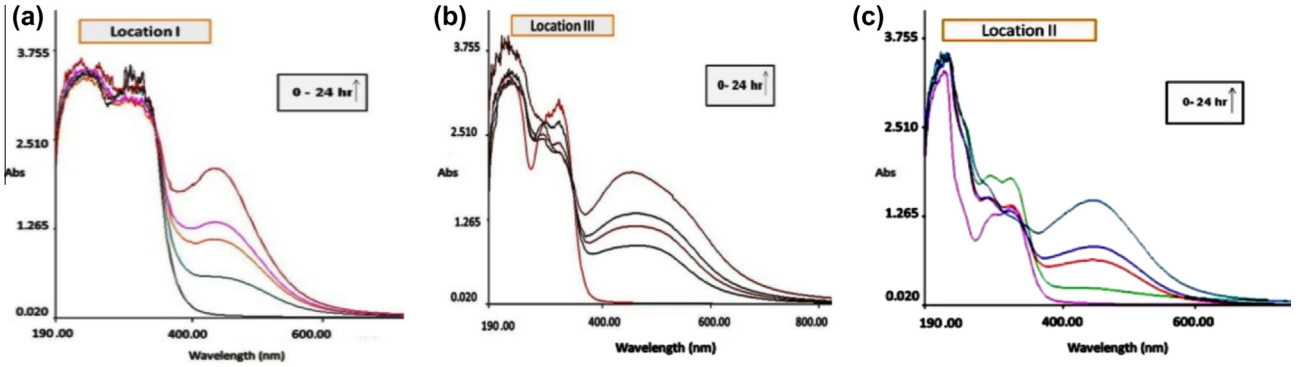

Figure 1 Typical UV–visible spectra of SNPs derived from the extracts of ipomoea (a) leaves, (b) stem and (c) roots, as a function of time.

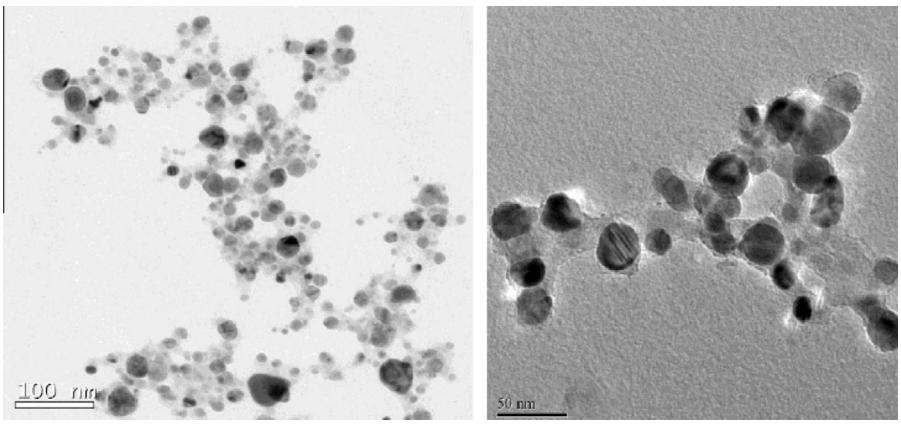

Figure 2 Spherical nanoparticles of fairly uniform (spherical) shape, but different, sizes formed by the extracts of ipomoea leaves (left) and of stem (right).

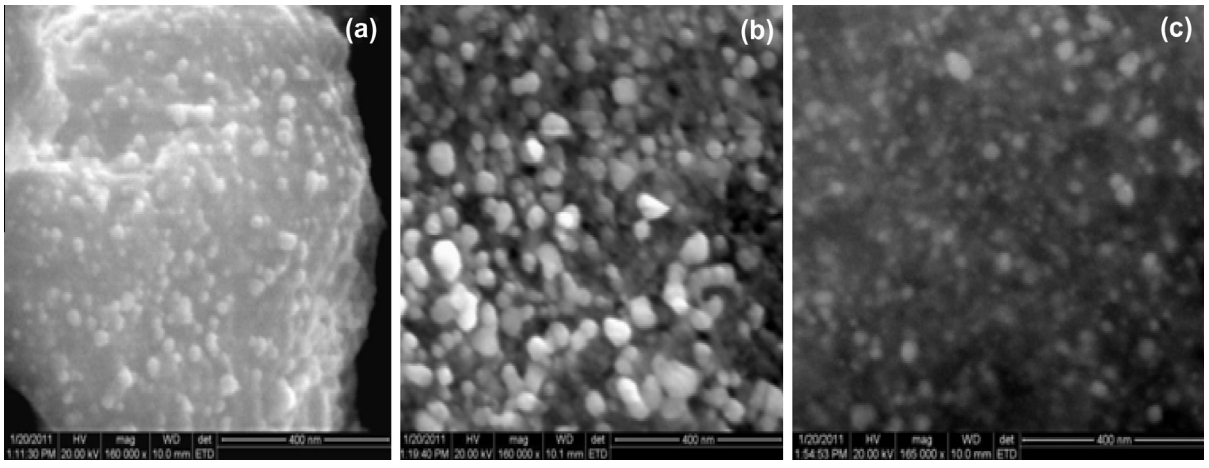

Figure 3 HR-SEM micrographs of SNPs generated using extracts of ipomoea (a) leaves, (b) stem and (c) root.

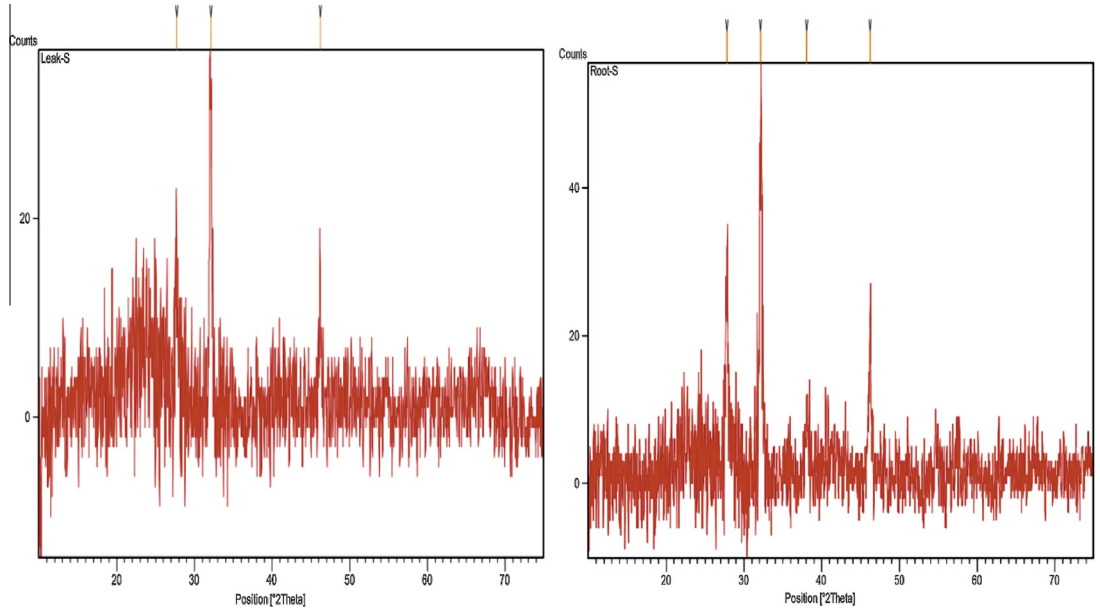

Figure 4 XRD images of SNPs generated using extracts of ipomoea leaf (left) and of root (right).

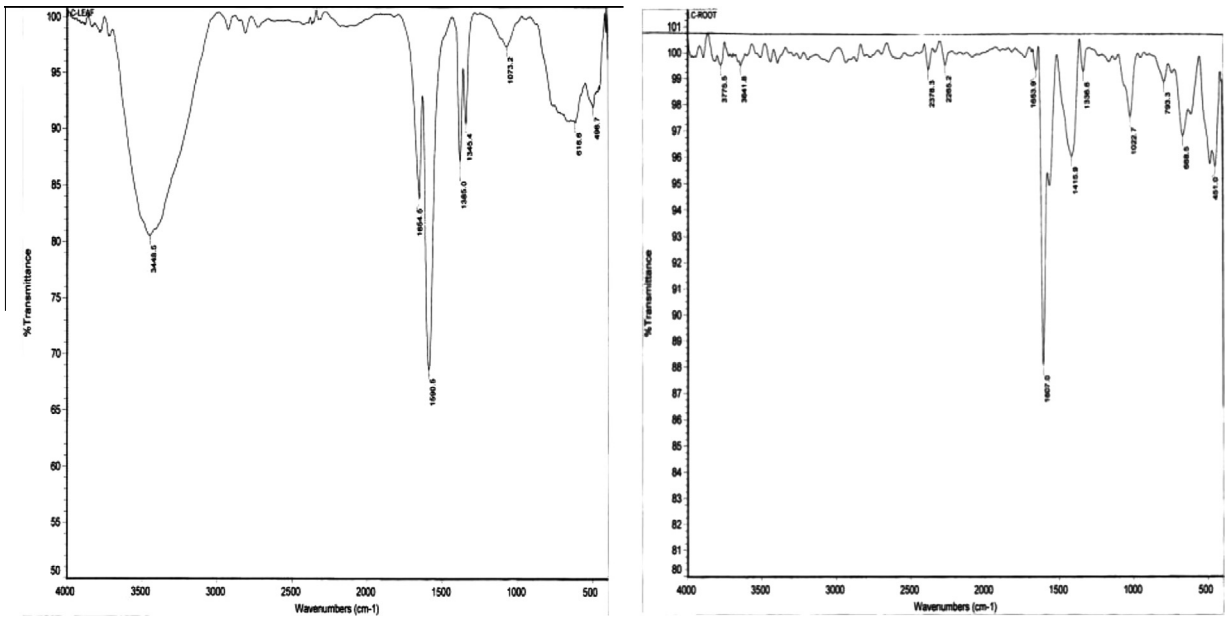

Figure 5 FTIR images of SNPs generated using extracts of ipomoea leaves (left) and of root (right).

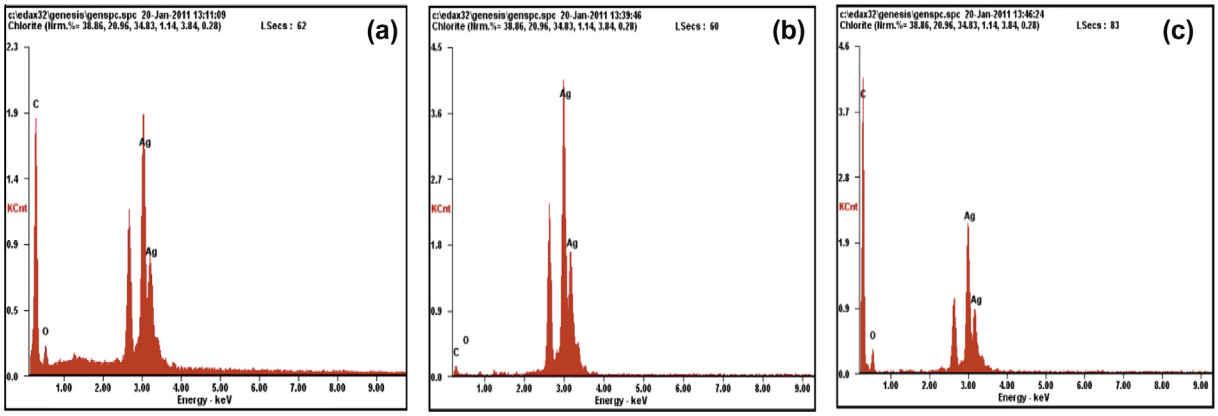

Figure 6 EDAX images of SNPs generated using extracts of ipomoea (a) leaves, (b) stem and (c) root.

Moreover, the shape of the spectra remained more or less unchanged with time (Fig. 1). This reveals that the patterns of polydispersion of nanoparticles and their shape isotropy did not change with time or with the source of ipomoea. Once the optical density at the λ_{max} had peaked, it remained constant for several days indicating that nanoparticles responsible for the peak had remained stable.

3.2. Characteristics of the SNPs

The synthesized SNPs were subjected to high-resolution scanning electron microscopy (HR-SEM) and transmission electron microscopy (TEM). Typical TEM and HR-SEM images are reproduced in Figs. 2 and 3, respectively.

X-ray diffractometry revealed the crystalline nature of the nanoparticles. Intense peaks were seen corresponding to (111), (200) and (220) Bragg's reflection based on the fcc crystal structure (Fig. 4).

Fourier transform infrared (FTIR) measurements revealed a strong band at 1654 cm^{-1} which corresponds to the stretching vibrations of amide C═O bands of proteins/polypeptides (Fig. 5). The bands at 1590 cm^{-1} and 1385 cm^{-1} correspond to carboxylates and C–N stretching of aromatic amino groups, respectively (Narayanan and Sakthivel, 2008). The bands at 1607 cm^{-1} and 1385 cm^{-1} correspond to C═C groups/aromatic rings (Das et al., 2010). Apparently the SNPs were stabilized by amide groups of proteins and the phenolic groups. Moreover, the fact that SNPs derived from different parts of ipomoea have similar FTIR profiles, indicates that similar biomolecules have been responsible for the reduction of silver ions and the stabilization of the resulting SNPs.

The energy dispersive X-ray (EDAX) spectra (Fig. 6) showed strong signals for silver, along with weak signals from few other elements like C and O. These signals could have arisen from proteins and enzymes that had stabilized the nanoparticles.

Table 4 Commonality and contrasts in the manner of SNP synthesis by ipomoea drawn from different locations and by different parts of ipomoea.

Aspect	SNPs synthesized using leaf extract	SNPs synthesized using stem extract	SNPs synthesized using root extract
Reproducibility	The metal–extract combinations of 1:7.5 and 1:15 gave reproducible results in terms of peak position and strength for all samples	The metal–extract combinations of 1:7.5 and 1:15 gave reproducible results in terms of peak position and strength for all the samples	The metal–extract combinations of 1:7.5 and 1:15 gave reproducible results in terms of peak position and strength for all samples
Peak position (λ_{max}) and intensity (absorbance)	The λ_{max} was in the range 432–459 nm and the absorbance was in the range 0.617–2.678	The λ_{max} was in the range 446–465 nm and the absorbance was in the range 0.849–1.968	The λ_{max} was in the range 429–452 nm and the absorbance was in the range 0.339–2.125
Bioreduction of Ag^+ to Ag^o	The formation of SNPs started at the 4th hr	In ipomoea of two locations, SNP formation started earlier than the ipomoea of the other two locations	The formation of SNPs, started at the 4th hr
Nature of SNPs	Narrow SPR band occurred in leaf extract indicating that the SNPs were monodispersed and spherical	Broad SPR band occurred in stem extract indicating that the SNPs were polydispersed	Initially a broad SPR band occurred indicating that nanoparticles were polydispersed. With time the SNPs the SPR band become narrow indicating that the SNPs gradually became monodispersed
	The rate of nanoparticle formation was greater when compared to SNPs formed by extracts of stem and root	The concentration and the rate of nanoparticle formation were lesser than the values for leaf and root	The concentration and the rate of nanoparticle formation were more when compared with stem but lesser when compared to leaves

Table 5 Degradation of the dye Alizarin Red S (1 ml of 7×10^{-4} M solution) in the absence or presence of SNPs (1 ml suspension), and 1 ml $NaBH_4$ (0.001 M) or H_2O_2 (0.1 M), in a total volume of 4 ml.

Reactants	Absorbance, at minutes			
	0	20	40	60
Dye + $NaBH_4$	1.25	1.00	0.94	0.94
Dye + $NaBH_4$ + SNPs	0.93	0.80	0.78	0.77
Dye + H_2O_2	1.60	1.60	1.58	1.56
Dye + H_2O_2 + SNPs	1.16	1.14	1.31	1.21

Table 6 Degradation of the dye Remozal Brilliant Blue R (1 ml of 3×10^{-4} M solution) in the absence or presence of SNPs (1 ml suspension), and 1 ml $NaBH_4$ (0.001 M) or H_2O_2 (0.001 M), in a total volume of 4 ml.

Reactants	Absorbance, at minutes					
	0	15	30	45	60	90
Dye + $NaBH_4$	0.43	0.41	0.40	0.38	0.38	0.36
Dye + $NaBH_4$ + SNPs	0.40	0.37	0.33	0.33	0.32	0.32
Dye + H_2O_2	0.44	0.42	0.42	0.42	0.42	0.42
Dye + H_2O_2 + SNPs	0.41	0.38	0.37	0.37	0.39	0.36

3.3. Effect of SNPs in catalyzing degradation of typical organic pollutants

The rate of degradation of Alizarin Red S and Remazol Brilliant Blue R dyes by $NaBH_4$ or H_2O_2 was monitored in the presence and absence of SNPs spectrophotometrically. SNPs are seen to catalyze the degradation, albeit slowly, under the conditions explored by us (Tables 5 and 6). This is reflected in faster lowering of dyes' absorbance in reactants containing the SNPs. The results establish the proof-of-concept.

4. Summary and conclusion

In perhaps the first-ever study of its type, effect of natural variability in the chemical composition of a botanical species on the synthesis of nanoparticles employing that specie's aqueous extract was explored. The plant species happened to be ipomoea (*I. carnea*) which is a major weed of the tropical and sub-tropical world, including India. The metal chosen was silver owing to the high demand of silver nanoparticles (SNPs) in several branches of technology (Abbasi et al., 2012a,b; Ghaffari-Moghaddam and Hadi-Dabanlou, 2014; Wang et al., 2014).

It was seen that, by-and-large, it is possible to identify metal–extract concentrations with which highly reproducible results *vis a vis* the shapes and sizes of SNPs can be achieved. Different plant parts—leaves, stem, and roots—give similar SNPs at certain metal–extract stoichiometries and dissimilar at some other. In this respect, too, fairly reproducible results were achieved when ipomoea drawn from different locations was used.

Proof-of-concept that SNPs can be used to catalyze degradation of complex organic pollutants was demonstrated with the examples of two dyes.

Acknowledgements

TA and SAA thank University Grants Commission (UGC), New Delhi for support in the form of a Major Research Project and SUG thanks the UGC for the award of Maulana Azad National Fellowship.

References

Abbasi, S.A., Abbasi, T., Anuradha, J., 2012a. A process for synthesis of bimetallic silver gold nanoparticles from weeds. Official Journal of the Patent Office 3, 944.

Abbasi, T., Neghi, N., Abbasi, S.A., 2012b. Gainful use of highly invasive terrestrial weed *Ipomoea carnea* for rapid and 'green' synthesis of silver nanoparticles. International Journal of Current Science 2, 57–62.

Anuradha, J., Abbasi, T., Abbasi, S.A., 2010. 'Green' synthesis of gold nanoparticles with aqueous extracts of neem (*Azadirachta indica*). Research Journal of Biotechnology 5 (1), 75–79.

Anuradha, J., Abbasi, T., Abbasi, S.A., 2011a. Biomimetic synthesis of gold nanoparticles using Aloe vera. International Journal of Environmental Science and Engineering Research 2 (1), 01–05.

Anuradha, J., Abbasi, T., Abbasi, S.A., 2011b. Rapid and reproducible 'green' synthesis of silver nanoparticles of consistent shape and size using *Azadirachta indica*. Research Journal of Biotechnology 6, 69–70.

Anuradha, J., Abbasi, T., Abbasi, S.A., 2014. Use of plants in biomimetic synthesis of gold nanoparticles. Journal of Nanoscience, in press.

Antony, J.J., Sithika, M.A.A., Joseph, T.A., Suriyakalaa, U., Sankarganesh, A., Siva, D., Kalaiselvi, S., Achiraman, S., 2013. In vivo antitumor activity of biosynthesized silver nanoparticles using Ficus religiosa as a nanofactory in DAL induced mice model. Colloids and Surfaces B 108, 185–190.

Awwad, A.M., Salem, N.M., Abdeen, A.O., 2013. Green synthesis of silver nanoparticles using carob leaf extract and its antibacterial activity. International Journal of Industrial Chemistry 4, 29.

Bhat, R., Ganachari, R., Ravindra, G., Venkataraman, A., 2013. Rapid biosynthesis of silver nanoparticles using Areca nut (Areca catechu) extract under microwave-assistance. Journal of Cluster Science 24, 107.

Chari, K.B., Sharma, Richa, Abbasi, S.A., 2005. Comprehensive Environmental Impact Assessment of Water Resources Projects, Volume 1. Discovery Publishing House, New Delhi, xvi + 580 pages.

Chari, K.B., Abbasi, S.A., 2005. A study of the aquatic and amphibious weeds of Oussudu lake. Hydrology Journal 28, 89–98.

Chari, K.B., Abbasi, S.A., 2004. Implications of environmental threats on the composition and distribution of fishes in a large coastal wetland. Hydrology Journal 27, 85–93.

Dahl, J.A., Maddux, B.L.S., Hutchison, J.E., 2007. Chemical Reviews 107, 2228–2269.

Das, R.K., Borthakur, B.B., Bora, U., 2010. Green synthesis of gold nanoparticles using ethanolic extract of *Centella asiatica*. Material Letters 64, 1445–1447.

Dubey, S.P., Dwivedi, A.D.D., Lahtinen, M., Lee, C., Kwon, Y., Sillanpaa, M., 2013. Protocol for development of various plants leaves extract in single-pot synthesis of metal nanoparticles. Spectrochimica Acta Part A: Molecular and Biomolecular Spectroscopy 103, 134–142.

Raspolli Galletti, A.M., Antonetti, C., Longo, I., Capannelli, G., Venezia, A.M., 2008. A novel microwave assisted process for the synthesis of nanostructured ruthenium catalysts active in the hydrogenation of phenol to cyclohexanone. Applied Catalysis, A: General 350, 46–52.

Raspolli Galletti, A.M., Antonetti, C., Giaiacopi, S., Piccolo, O., Venezia, A.M., 2009. Innovative process for the synthesis of nanostructured ruthenium catalysts and their catalytic performance. Topics in Catalysis 52 (8), 1065–1069.

Raspolli Galletti, A.M., Antonetti, C., Venezia, A.M., Giambastiani, G., 2010. An easy microwave-assisted process for the synthesis of nanostructured palladium catalysts and their use in the selective hydrogenation of cinnamaldehyde. Applied Catalysis, A: General 386 (1–2), 124–131.

Raspolli Galletti, A.M., Toniolo, L., Antonetti, C., Evangelisti, C., Forte, C., 2012. New palladium catalysts on polyketone prepared through different smart methodologies and their use in the hydrogenation of cinnamaldehyde. Applied Catalysis, A: General 447–448, 49–59.

Raspolli Galletti, A.M., Antonetti, C., Marracci, M., Piccinelli, F., Tellini, B., 2013. Novel microwave-synthesis of Cu nanoparticles in the absence of any stabilizing agent and their antibacterial and antistatic applications. Applied Surface Science 280, 610–618.

Gavhane, A.J., Padmanabhan, P., Kamble, S.P., Jangle, S.N., 2012. Synthesis of silver nanoparticles using extract of neem leaf and Triphala and evaluation of their antimicrobial activites. International Journal of Pharma and Bio Sciences 3, 88–100.

Gorniak, S., Gotardo, A., Pfister, J., 2010. The effects of *Ipomoea carnea* on neonate behavior: a study in goats. Toxicology Letters 196, S186.

Ghaffari-Moghaddam, M., Hadi-Dabanlou, R., 2014. Plant mediated green synthesis and antibacterial activity of silver nanoparticles using *Crataegus douglasii* fruit extract. Journal of Industrial and Engineering Chemistry 20 (2), 739–744.

Hueza, I.M., Guerra, J.L., Haraguchi, M., Asano, N., Górniak, S.L., 2005. The role of alkaloids in Ipomoea carnea toxicosis: a study in rats. Experimental and Toxicologic Pathology 57 (1), 53–58.

Ikeda, K., Kato, A., Adachi, I., Haraguchi, M., Asano, N., 2003. Alkaloids from the poisonous plant *Ipomoea carnea*: effects on intracellular lysosomal glycosidase activities in human lymphoblast cultures. Journal of Agricultural and Food Chemistry 51 (26), 7642–7646.

Kotakadi, S.V., Gaddam, S.A., Rao, Y.S., Prasad, K.V., Reddy, A.V., Sai Gopal, D.V.R., 2014. Biofabrication of silver nanoparticles using *Andrographis paniculata*. European Journal of Medicinal Chemistry 73, 135–140.

Kumar, K.P., Paul, W., Sharma, C.P., 2012. Green synthesis of silver nanoparticles with *Zingiber officinale* extract and study of its blood compatibility. BioNanoScience.

Kumar, K.M., Mandal, B.K., Kumar, K.S., Reddy, P.S., Sreedhar, B., 2013. Biobased green method to synthesise palladium and iron nanoparticles using *Terminalia chebula* aqueous extract. Spectrochimica Acta Part A: Molecular and Biomolecular Spectroscopy 102, 128–133.

Meira, M., DeSilva, E.P., David, J.M., David, J.P., 2012. Review of the genus Ipomoea: traditional uses, chemistry and biological activities. Brazilian Journal of Pharmacogenesis 22, 682–713.

Narayanan, K.B., Sakthivel, N., 2008. Coriander leaf mediated biosynthesis of gold nanoparticle. Materials Letters 62, 4588–4590.

Nazeruddin, G.M., Prasad, N.R., Waghmare, S.R., Garadkar, K.M., Mulla, I.S., 2014. Extracellular biosynthesis of silver nanoparticle using *Azadirachta indica* leaf extract and its anti-microbial activity. Journal of Alloys and Compounds 583, 272–277.

Shankar, S.S., Ahmad, A., Parsricha, R., Sastry, M., 2003. Bioreduction of chloroaurate ions by geranium leaves and its endophytic fungus yields gold nanoparticles of different shapes. Journal of Materials Chemistry 13, 1822–1826.

Shankar, S.S., Ahmad, A., Pasricha, R., Khan, M.I., Kumar, R., Sastry, M., 2004. Immobilization of biogenic gold nanoparticles in thermally evaporated fatty acid and amine thin films. Journal of Colloid and Interface Science 274, 69–75.

Wang, T., Jin, X., Chen, Z., Megharaj, M., Naidu, R., 2014. Green synthesis of Fe nanoparticles using eucalyptus leaf extracts for treatment of eutrophic wastewater. Science of the Total Environment 466–467, 210–213.